Bioelectrochemistry 73 (2008) 55–63

Contents lists available at ScienceDirect

Bioelectrochemistry

journal homepage: www.elsevier.com/locate/bioelechem

Spectroelectrochemical study of hemoglobin A, alpha- and beta-fumarate crosslinked hemoglobins; implications to autoxidation reaction

Simona A. Dragan [a], Kenneth W. Olsen [a], Edwin G. Moore [b], Alanah Fitch [a,*]

[a] Department of Chemistry, Loyola University Chicago, 1068 W. Sheridan Rd., Chicago, Il. 60626, United States
[b] Baxter Healthcare Corporation, One Baxter Parkway, Deerfield, Il. 60015-4625, United States

ARTICLE INFO

Article history:
Received 8 March 2007
Received in revised form 31 March 2008
Accepted 9 April 2008
Available online 16 April 2008

Keywords:
Hemoglobin
Fumarate crosslinked hemoglobin
Spectroelectrochemistry
Formal redox potentials
Oxidation kinetics

ABSTRACT

The thermodynamics and kinetics of the reaction DeoxyHb-Fe^{2+} ↔ MetHb-Fe^{3+} for human hemoglobin A (HbA), alpha- and beta-fumarate crosslinked hemoglobins were investigated by spectroelectrochemistry. Information from this study is used to determine what structural features and experimental conditions stabilize ferrous *vs.* ferric form of hemoglobin, and what implications this stabilization may have on the autoxidation reaction. Alpha- and beta-fumarate crosslinked hemoglobins, αXL-HbA and βXL-HbA, were obtained by crosslinking deoxyhemoglobin and oxyhemoglobin, respectively, with bis(3,5-dibromosalicyl) fumarate (DBSF). Formal redox potentials, E^0, and reduction/oxidation rates were measured in the presence of mediator, hexammineruthenium(III) chloride. It was found that E^0 shifted positive for the alpha-, and negative for the beta-fumarate crosslinked hemoglobin compared to HbA for all experimental conditions investigated. This shift was consistent with stabilization of the tense (positive shift) or relaxed conformation (negative shift) conferred by crosslinking. Formal redox potentials shifted positive with addition of nitrate and chloride ions for αXL-HbA, indicating additional stabilization of the T quaternary. The slopes of the Nernst plots showed evidence of cooperativity as expressed by n_{max}. The data points (E^0, n_{max}) were fitted by the MWC model which states that the electron transfer and the addition/removal of water are concerted. The set of K_R and c values, where the parameter c is the ratio K_R/K_T and K_R and K_T are the ligand (water molecule and an electron–hole) dissociation constants for the R and T states, for the beta-crosslinked hemoglobin compared to that of HbA and alpha-crosslinked hemoglobin indicated that crosslinking of oxyhemoglobin affected differently the inner-coordination sphere at the heme site. By modulating the electrolyte concentration the reduction rates were measured as a function of ΔE^0, the difference in E^0 between hemoglobin molecules and mediator. Linearization of the Marcus cross-relationship (based on the concerted water and electron transfer) was good for HbA, and poor for αXL-HbA and βXL-HbA, consistent with results obtained by the MWC analysis. This may imply that the reduction of HbA is controlled by the driving force, ΔE^0, whereas the reduction of αXL-HbA and βXL-HbA occurs by a non-concerted mechanism controlled by structural features brought about by crosslinking. The autoxidation reaction, conversion of oxygen-bound ferrous hemoglobin to ferric hemoglobin, was found independent of E^0. Alpha-fumarate crosslinked hemoglobin showed the highest autoxidation rate despite its positive shift in formal redox potential as compared to HbA, followed by beta-fumarate crosslinked hemoglobin, and by native hemoglobin. These data suggest that the chemical mechanism of oxygen dissociation and accessibility of water and oxygen radicals to heme site control autoxidation.

1. Introduction

The main component of the red blood cells, hemoglobin A (HbA), functions as an efficient oxygen carrier by reversibly binding oxygen at the ferrous ion of the heme groups [1]. The heme groups are embedded in each of the two alpha and two beta globin chains that form the molecule. In addition to regulating oxygen affinity, the globin structure serves to keep the heme complex in the reduced state.

Binding and releasing of oxygen as well as oxidation takes place at the iron ion of the heme group. In deoxyhemoglobin penta-coordinated Fe^{2+} is out of the porphyrin plane (protoporphyrin IX) on the distal side by 0.06 nm. Upon binding oxygen the ferrous ion moves into the porphyrin plane. Similarly, iron comes close to the porphyrin plane (by 0.021 nm) upon oxidation and adds water at the sixth coordination position. Changes at the heme group are accompanied by changes in the overall conformation. Following oxygen binding or oxidation, the hemoglobin tetramer shifts its conformation from tense

* Corresponding author. Tel.: +1 773 508 3119; fax: +1 773 508 3086.
E-mail address: afitch@luc.edu (A. Fitch).

1567-5394/$ – see front matter © 2008 Elsevier B.V. All rights reserved.
doi:10.1016/j.bioelechem.2008.04.013

(T) to relaxed (R). The biggest conformational change takes place at the β–β interface, which is at the closest approach in methemoglobin or oxyhemoglobin and 0.6 nm apart in deoxyhemoglobin [1]. Upon oxidation, hemoglobin loses its capability of binding oxygen. Although loss of electrons occurs spontaneously *in vivo*, the oxygen binding state is restored by electron-donating systems. However, activated oxygen species can be formed in the process, with potentially adverse effects [2].

The oxidation–reduction studies of hemoglobin performed by spectroelectrochemistry (SEC) were found to provide insight into the electron transfer process of the molecule, more specifically into the influence of electronic factors on the heme group and interaction between subunits. Bonaventura, Crumbliss and co-workers found that a sixth ligand bound to iron could alter the redox behavior of hemoglobin in different ways as the electron density at the heme is varied [3–8]. Ligands with strong electron donor capabilities stabilized the ferric ion shifting the formal redox potential negative. The magnitude and direction of shifts in formal redox potential were found to be fine-tuned by the nature and concentration of allosteric effectors (anions). The effect of anions was attributed to stabilization of one conformation relative to the other which indirectly changes the electron density and steric environment at the heme iron.

Using a spectroelectrochemical method designed in our laboratory we explored the redox behavior of two hemoglobins crosslinked with bis(3,5-dibromosalicyl) fumarate (DBSF) compared to that of HbA. When the crosslinking reaction is carried out on oxyhemoglobin, DBSF binds between ε-amino groups of Lys 82 on the EF corner of the β chains, resulting in β-fumarate crosslinked hemoglobin or βXL-HbA [9]. The same crosslinker binds between Lys 99 (FG corner) of the α chains when the modification is carried out on deoxyhemoglobin resulting in α-fumarate crosslinked hemoglobin or αXL-HbA [10]. Crosslinking at the α–α interface stabilizes the tense (T) quaternary conformation while crosslinking at the β–β interface stabilizes the R conformation. Stabilizing either the T or R conformations causes changes in oxygenation [9,10]. βXL-HbA shows an increased oxygen affinity and diminished control of oxygen binding by anions because the central cavity charge and shape have been altered [11]. Crosslinking at the $\alpha_1\alpha_2$ interface conferred on αXL-HbA an oxygen affinity close to that of blood, making it a good candidate as a blood substitute [12]. Crosslinked hemoglobins are snap-shots of the transition T↔R, which bring about structural changes at the heme site [13] that may concurrently alter ligand approach to the binding site by steric factors. The modified electron density at the heme iron is expected to have an impact on the redox behavior of αXL- and βXL-HbA, that will be expressed by shifts in the formal redox potential and changes in redox cooperativity.

This paper focuses on the thermodynamics and kinetics of the oxidation/reduction reactions of hemoglobin, αXL- and βXL-HbA. The effect of allosteric effectors, chloride and nitrate ions on formal redox potential and reduction rates is investigated. Self-exchange rate constants calculated based on the Marcus cross-relationship are correlated with structural changes that occur during the oxidation/reduction reactions of hemoglobin and crosslinked hemoglobins. This work explores the structural features and conditions likely to confer stabilization of Fe^{2+} in the redox reactions. The findings are used to investigate whether such stabilization affects the autoxidation reaction.

2. Experimental

Hemoglobin A was isolated as in the method of Dozy, Kleihauer and Huisman from outdated packed red blood cells (RBC) obtained from LifeSource [14]. Anion-exchange chromatography on a DEAE (diethylaminoethyl) Sephadex resin was used for hemoglobin purification from hemolysate solution. The hemoglobin was eluted with a pH gradient established between solutions of Trizma/KCN pH 8.5 and pH 7.2, respectively. Hemoglobin A was the second fraction eluted from the column, after HbA2, and before glycosylated HbA (HbAIc), as identified by alkaline agarose gel electrophoresis. The purified HbA solution was concentrated by ultrafiltration over an Amicon PM30 membrane. Concentrated hemoglobin samples used in SEC and autoxidation experiments were additionally dialyzed against 0.01 M MOPS, pH 7.1, to remove any traces of cyanide. The concentration of hemoglobin was determined spectrophotometrically in the UV–Vis region based on the method of Winterbourn [15]. Hemoglobin samples freshly eluted from the column and immediately concentrated had OxyHbA in excess of 98%, and hemichrome formation did not occur. Hemoglobin A prepared and purified with this method was used immediately for crosslinking, SEC and autoxidation experiments without further purifications. The final concentration of stock hemoglobin samples was 1 to 2 mM/heme.

αXL-HbA was a generous gift from Baxter Healthcare Corporation. Prior to use the αXL-HbA was dialyzed against MOPS 0.01 M, pH 7.1 for 24 h. Stock samples were stored at −80 °C for long period of times. Samples for the ongoing experiments were kept at 4 °C. The percentage of met form was found less than 1% and no further purification was needed.

βXL-HbA was obtained according to the method of White and Olsen [16]. The crosslinker, DBSF, was synthesized according to the procedure outlined by Walder et al. [17]. Anion-exchange chromatography was used to purify βXL-HbA from the reaction mixture consisting of crosslinked and uncrosslinked hemoglobins. The purity and molecular weight of the eluted fractions were determined by alkaline agarose electrophoresis and SDS-PAGE (sodium dodecylsulfate polyacrylamide gel electrophoresis). The fraction containing the βXL-HbA was dialyzed against MOPS 0.01 M, pH 7.1 and later concentrated by ultrafiltration over an Amicon PM30 membrane. Sample concentration was determined spectrophotometrically for hemoglobin A. Samples consisted of 90 to 95% Oxy, 5 to 10% Met, and, occasionally hemichrome. Those samples containing measurable amounts of hemichrome were discarded. For the autoxidation experiments the βXL-HbA was needed to be converted to the ferrous Oxy state using the dithionite procedure as described in the literature [18].

MOPS, 3-[*N*-morpholino] propanesulfonic acid (Sigma), $Ru(NH_3)_6Cl_3$ (ALFA-Aesar), and myoglobin (lyophilized solid from horse skeletal muscle — Sigma) were used as received. Deionized water was used in all experiments. Stock solutions of electrochemical mediator were prepared by dissolving $Ru(NH_3)_6Cl_3$ in the desired buffer/electrolyte solution. The concentration of mediator and the concentration of buffer/electrolyte were twice of that employed in SEC experiments. The stock mediator/buffer/electrolyte solutions were stored at 4 °C, and were purged with nitrogen prior to use. For a given experiment, calculated volumes of degassed deionized water and of concentrated hemoglobins were added to the stock solution of mediator/buffer/electrolyte in such a way to bring the concentration of all species to the desired values. Other chemicals, potassium ferricyanide ($K_3Fe(CN)_6$) from Fisher (>99%), DCPIP (dichlorophenolindophenol) and the electrolytes KCl and $NaNO_3$ (from Aldrich), were used as received.

SEC was carried out in an optically transparent thin layer electrochemical cell (OTTLE) designed in our laboratory. A closed thin layer chamber was made between two quartz plates, 25×75×3 mm^3 (Quartz Plus, Inc., Brookline NH), separated by a Teflon spacer. The inner cell compartment volume was 225 μL and the thickness was 0.5 mm. The unique features of this cell include the symmetrical double counter electrode (CE) placement to reduce ohmic drop across the cell and the use of a platinum minigrid (52 lines/in, Fisher) as a working electrode (WE), which allows for rapid electrolysis within the cell. Potentials were measured *vs.* a miniature Ag/AgCl reference electrode (RE), housed in its own compartment. The RE compartment was sealed to OTTLE thus ensuring the oxygen-free environment necessary for the redox studies of hemoglobin and crosslinked hemoglobins. The working electrode was cleaned electrochemically by

stepping the potential to either −0.4 V or +1.6 V and maintaining the potential at these extreme values for 1 to 3 min. This procedure was repeated at least three times. When the potential was kept at −0.4 V the cell was filled with 0.1 M H_2SO_4 while at +1.6 V the cell was filled with 0.1 M NaOH. Between potential steps the cell was rinsed several times with deionized water.

The performance of the cell was verified against well characterized redox systems such as $Fe(CN)_6^{3-/4-}$, 2,6-dichlorophenolindophenol (DCPIP), and myoglobin. Good agreement of our experimental data obtained by spectroelectrochemistry with literature data under similar experimental conditions was obtained. The following values, *vs.* NHE, represent our work followed in parentheses by literature data. SEC on $Fe(CN)_6^{3-/4-}$/KCl 0.2 M yielded E^0 of 0.438 V(0.449 V) and n of 0.97 (0.95) compared to data at Au minigrid in NaCl 0.5 M [35]. For DCPIP/NaCl 0.1 M, phosphate buffer 0.1 M, pH 7 we obtained E^0 of 0.228 V (0.227 V) and n of 1.83 (1.88) compared to data at a gold minigrid [19]. Myoglobin in the presence of mediator, $Ru(NH_3)_6Cl_3$, with $NaNO_3$ 0.2 M, MOPS 0.05 M, pH 7.1 yielded E^0=0.042 V (0.037 V) and n of 0.87 (0.95) [20]. Myoglobin with mediator $Ru(NH_3)_6Cl_3$ in phosphate buffer 0.2 M, pH 7.0 yielded E^0=0.037 V (0.047 V) and n of 1.0 (0.95) [21].

An EG&G PARC (Princeton Applied Research) three-electrode potentiostat model 273 was used for electrochemical measurements. The potentials were measured against the reference electrode Ag/AgCl immersed in the background electrolyte solution. The auxiliary and working electrodes consisted of platinum wire and platinum minigrid, respectively. When conventional cyclic voltammetry was needed for evaluation of E^0, the potentials were measured against the saturated calomel electrode (SCE) and the working electrode consisted of a platinum disc.

A Hewlett-Packard diode array spectrophotometer model 8453 was used for UV–Vis measurements. The OTTLE was placed in the sample compartment in its own holder, and aligned in the optical path of the spectrophotometer. Nitrogen lines were connected to the cell for degassing prior to starting the experiment. The same nitrogen lines were used simultaneously for degassing of the electrolyte and reference electrode filling solutions.

An oxygen-free environment was needed to study the equilibrium $Deoxy(Fe^{2+}) \leftrightarrow Met(Fe^{3+})$ without side reactions due to dissolved or freed oxygen. However, hemoglobin and crosslinked hemoglobin samples were found to contain mainly oxyhemoglobin (>98%). The bound oxygen, as well as traces of oxygen dissolved in the electrolyte solution, was removed by imposing an initial negative potential on the system (usually −0.5 V *vs.* Ag/AgCl). At this potential a 555 nm peak characteristic for deoxyhemoglobin appeared and the peaks at 540 nm and 576 nm characteristic for oxyhemoglobin disappeared (Fig. 1a) [15]. These peaks do not reappear throughout the spectroelectrochemical experiment, whether applying oxidative or reductive potentials (Fig. 1b), confirming the oxygen-free environment provided by the OTTLE cell.

SEC experiments were usually performed in the reductive direction first. After an initial negative imposed potential at −0.5 V *vs.* Ag/AgCl the potential was stepped to +0.3 V thus oxidizing all ferrous hemoglobins. From this value potential steps were applied in the reductive direction, each time from the previous value in increments of 50 to 10 mV until hemoglobin is completely reduced (to −0.5 V *vs.* Ag/AgCl). Then, the experiment was continued in the oxidative direction in a similar manner. The time needed for complete reduction of ferric and oxidation of ferrous hemoglobins in a single step was about 5 to 10 min, and 15 to 20 min, respectively. Spectra were recorded at every applied potential step after solution equilibrium was reached. The Soret absorbance bands of hemoglobin solutions were used for evaluation of data.

Formal redox potentials of myoglobin and hemoglobins were evaluated against the Ag/AgCl reference electrode immersed in electrolyte/buffer solution in the OTTLE cell. The potentials were

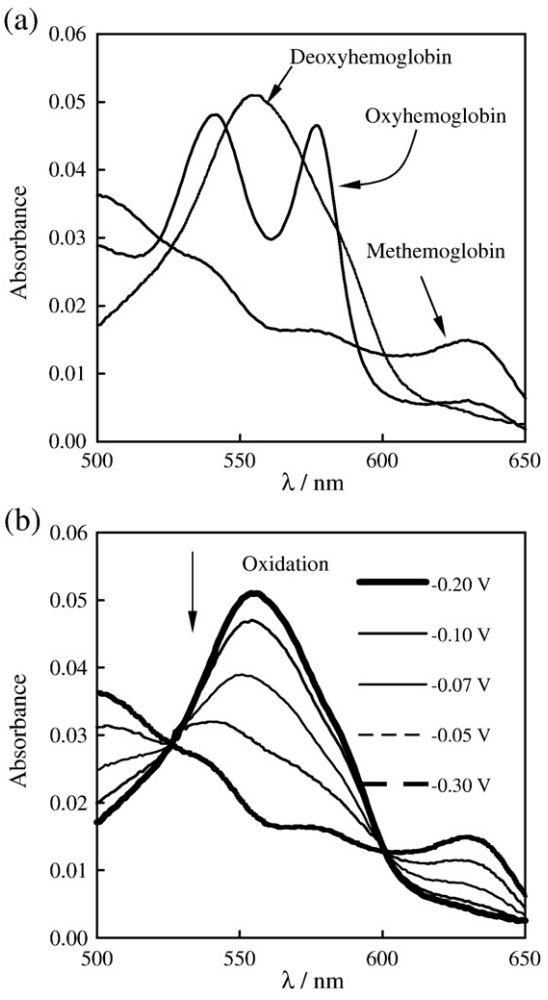

Fig. 1. (a) Spectra of oxyhemoglobin, deoxyhemoglobin and methemoglobin. A negative potential imposed on the system (−0.5 V *vs.* Ag/AgCl) causes the initial peaks at 540 and 576 nm characteristic for oxyhemoglobin to disappear while the peak at 555 nm characteristic for deoxyhemoglobin is formed. A small peak at 630 nm appears when all hemoglobin is in oxidized form (methemoglobin). (b) Spectra recorded at different oxidation–reduction stages (the applied potential is measured *vs.* Ag/AgCl electrode). Note that the peaks at 540 and 576 nm do not reappear throughout the redox experiment.

then corrected with respect to the E^0 of $Ru(NH_3)_6^{3+/2+}$ obtained by thin layer cyclic voltammetry under the same experimental conditions (Table 1). The difference between the values of the formal redox potential of $Ru(NH_3)_6^{3+/2+}$ measured by thin layer CV in the OTTLE cell and by conventional CV was added to the value of E^0 of hemoglobin or myoglobin determined in the OTTLE cell.

The formal redox potential, E^0, was determined as the average of the anodic and cathodic peak potentials in cyclic voltammetry (Fig. 2).

Kinetic measurements were performed for hemoglobin and crosslinked hemoglobins in the OTTLE cell by recording absorbance changes upon applying large potential steps from −0.5 V to +0.3 V *vs.* Ag/AgCl and vice versa. The wavelengths used for monitoring were 406, 430 and 555 nm, as for equilibrium redox measurements.

The autoxidation of 0.1 mM/heme solution of hemoglobins was followed by measuring changes in the hemoglobin spectrum at room temperature according to the method of Winterbourn [15]. Absorbance changes were recorded every 2 h in the beginning and 4 to 8 h after the first two days for each sample, from 500 to 750 nm with an HP 8451A diodearray spectrophotometer. The total time for each experiment was 10 days.

The formal redox potential, E^0, was determined as the average of the anodic and cathodic peak potentials in cyclic voltammetry. E^0 and

Table 1
Experimental and literature values for formal redox potential, E^0 (*vs.* NHE unless otherwise specified) and number of electrons transferred, n, for the $Ru(NH_3)_6^{3+/2+}$ couple determined by conventional and thin layer cyclic voltammetry (CV) and controlled potential coulometry (CPC) in various electrolyte/buffer systems

System	Method	This work	Literature
$Ru(NH_3)_6Cl_3$ 0.5–1 mM	CPC	E^0=0.077 V	
KCl 0.2 M,	WE: glassy carbon	n=0.93	
MOPS 0.05 M, pH 7.1	CPC (OTTLE)	E^0=0.072 V	
	WE: Pt minigrid		
	Thin layer CV	E^0=0.048 V	
	WE: glassy carbon	n=0.89	
	Thin layer CV (OTTLE)	E^0=0.051 V	E^0=−0.150 V *vs.*
	WE: Pt minigrid		Ag/AgCl [20]
$Ru(NH_3)_6Cl_3$	CV	E^0=0.047 V	E^0=−0.150 V *vs.*
KCl 0.2 M	WE: Pt		Ag/AgCl [20]
MOPS 0.05 M, pH 7.1			
$Ru(NH_3)_6Cl_3$	CV	E^0=0.054 V	
KCl 0.05 M	WE: Pt		
MOPS 0.05 M, pH 7.1			
$Ru(NH_3)_6Cl_3$	CV	E^0=0.050 V	
$NaNO_3$ 0.2 M	WE: Pt		
MOPS 0.05 M, pH 7.1			
$Ru(NH_3)_6Cl_3$	CV	E^0=0.056 V	
$NaNO_3$ 0.05 M	WE: Pt		
MOPS 0.05 M, pH 7.1			
$Ru(NH_3)_6Cl_3$	CV	E^0=0.068 V	
MOPS 0.05 M, pH 7.1	WE: Pt		

The experimental values presented are the average of at least three measurements. Standard deviation for E^0 was between ±2 and ±4 mV, and that for n was ±0.05.

electron stoichiometry, n, are determined from SEC by applying the Nernst equation:

$$\log\frac{[O]}{[R]} = n\frac{2.3F}{RT}(E - E^0) \quad (1)$$

[O] and [R] represent the concentration of the oxidized and reduced species, respectively, and R, T and F have their usual meanings.

[O]/[R] at any given applied potential, E, is:

$$\left(\frac{[O]}{[R]}\right)_E = \frac{A_{red} - A_E}{A_E - A_{ox}}, \quad (2)$$

where A_{red} is the absorbance of the completely reduced species, A_E is the absorbance at the applied potential E, and A_{ox} is the absorbance of the completely oxidized species, all determined at the same wavelength. The first derivative of the Nernst plot with respect to potential,

$$n = \frac{RT}{2.3F}\frac{d[\log([O]/[R])]}{dE} \quad (3)$$

yields two significant n values: n_{50} (at E^0) and n_{max} (maximum along the Nernst plot).

First rate order reduction and autoxidation constants were evaluated according to the following equation [22]:

$$\ln(A_t - A_\infty) = -kt + \ln(A_0 - A_\infty), \quad (4)$$

where A_t is the absorbance at a set wavelength at time t, A_0 and A_∞ are the initial and final absorbances, respectively.

3. Results and discussion

3.1. Formal redox potentials

A typical spectroelectrochemical experiment is illustrated in Fig. 3a. The redox process is chemically reversible for HbA, αXL- and βXL-HbA in the reductive and oxidative directions, whether the processes were monitored at 406 or 430 nm (Fig. 3b). Fig. 3a illustrates the characteristics changes in UV–Vis spectra for deoxy (reduced) and met (oxidized) hemoglobin. The conversion between the two forms

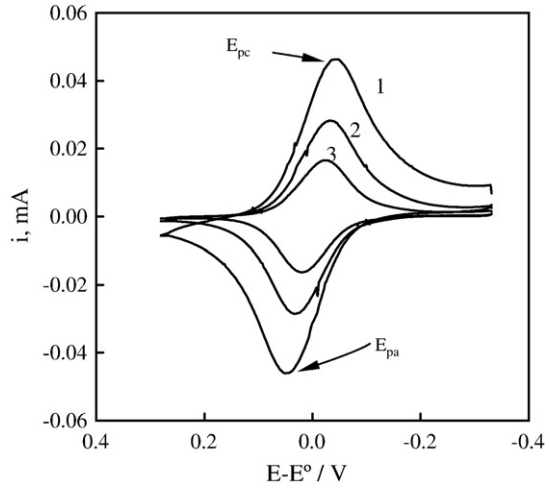

Fig. 2. Thin layer cyclic voltammograms of $Ru(NH_3)_6^{3+/2+}$ in KCl 0.2 M, MOPS 0.05 M, pH 7.1 at scan rates of: (1) 2 mV/s, (2) 1 mV/s, and (3) 0.5 mV/s. Initial concentration of electroactive species is 0.5 mM, the volume of thin layer cell is V=50 µL. The separation between peak potentials, $\Delta E_p = E_{pc} - E_{pa}$, is 43 mV at 0.5 mV/s. The formal redox potential is E^0=0.051 V *vs.* NHE and it is calculated as the average of E_{pa} and E_{pc}.

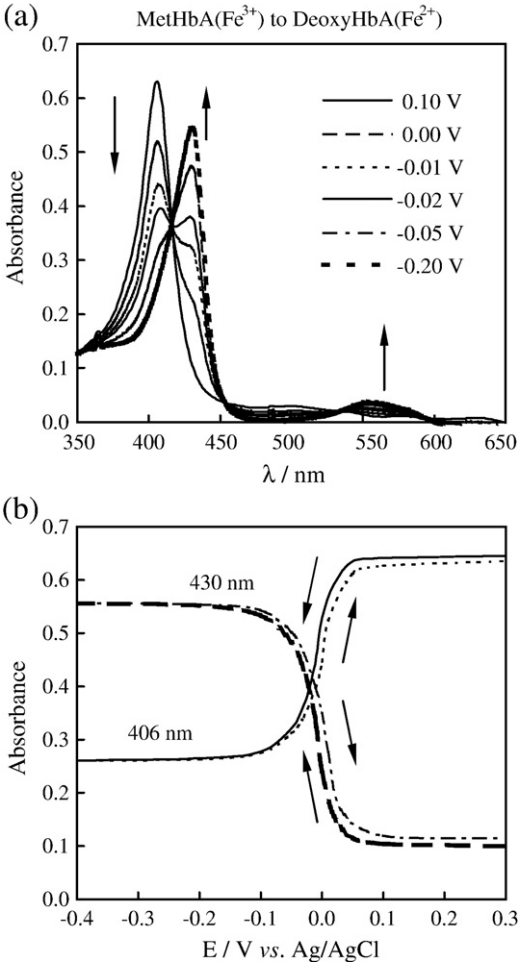

Fig. 3. Spectroelectrochemistry of hemoglobin A (0.1 mM/heme) in the presence of Ru $(NH_3)_6Cl_3$ 0.5 mM, KCl 0.2 M, MOPS 0.05 M, pH 7.1: (a) spectra recorded at different potentials (measured against Ag/AgCl) during reduction of MetHbA to DeoxyHbA; (b) absorbance monitored at 406 nm and 430 nm *vs.* applied potential for reduction (continuous lines) and oxidation (dotted lines) reactions.

can be followed by a decrease in absorbance by deoxyhemoglobin (406 nm) or by an increase in absorbance by methemoglobin (430 nm). A plot of absorbance *vs.* potential (Fig. 3b) shows that the process is reversible as data for reduction can be superimposed over data for oxidation. The very slight discrepancy observed is attributed to electrolyte/buffer solution resistance arising from the ohmic drop across the thin layer cell. The ohmic drop calculated from solvent resistance and cell characteristics is between 5 and 11 mV consistent with the variation around the end point of the titrations. The absorbance data was transformed to concentration via Eq. (2) and plotted as a Nernst plot (Eq. (1)) in Fig. 4a. Superimposition of Nernst plots obtained by applying reductive and oxidative potential steps was observed. The formal redox potentials measured for reduction and oxidation agree within 3 to 10 mV. Experimental results compared with literature values for HbA, αXL- and βXL-HbA are summarized in Table 2.

As seen in Fig. 4a, the shape of Nernst plots was sigmoidal for hemoglobin and crosslinked hemoglobins in both oxidation and reduction experimental approaches, in contrast to the straight line obtained for myoglobin (not shown). The non-linear aspect of the Nernst curve can be better seen through the plot of its first derivative (Fig. 4b) with respect to potential (Eq. (3)). The Nernst plot is analogous to a Hill plot so that the slope gives a value of n [4]. In the first case this n is the Nernst coefficient, which is a measure of the cooperativity of electron transfer. In the second case it is the Hill coefficient, which is a measure of the cooperativity of ligand binding. Similarity in these two coefficients may indicate that the same structural conformational changes are responsible for the cooperativity of ligand binding and electron transfer.

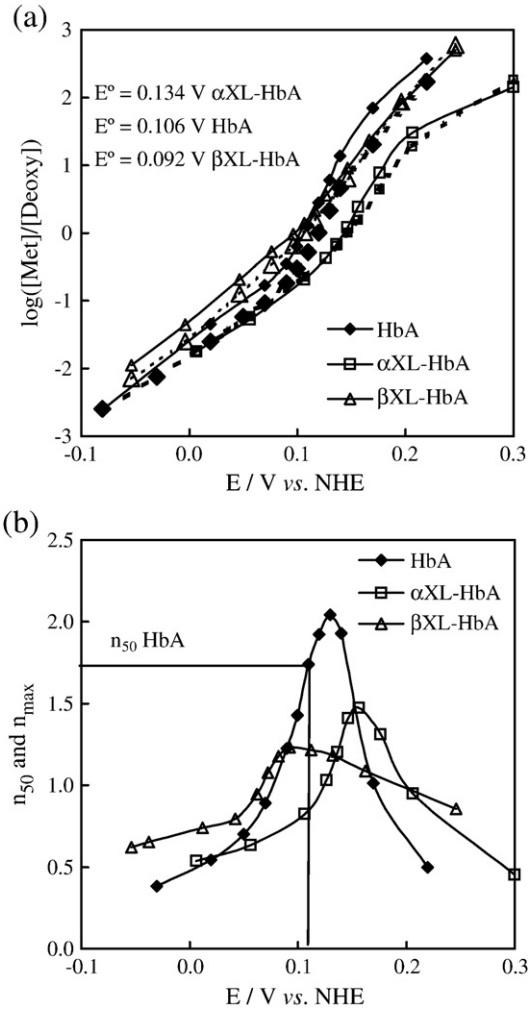

Fig. 4. (a) Nernst representations for HbA (406 nm), αXL-HbA (430 nm) and βXL-HbA (555 nm) for reduction (continuous lines) and oxidation (dotted lines). Experimental conditions: sample concentration 0.1 mM/heme, $Ru(NH_3)_6Cl_3$ 0.5 mM, MOPS 0.05 M, pH 7.1; (b) first derivative of the Nernst curves shown in (a) — average of reduction and oxidation.

Table 2
Formal redox potential, E^0, (*vs.* NHE), n_{50} and n_{max} for HbA, αXL-HbA, and βXL-HbA determined by spectroelectrochemistry (SEC)

System	Literature	This work	This work	This work
	HbA	HbA	αXL-HbA	βXL-HbA
MOPS 0.05 M, pH 7.1	E^0 = 0.098 V	E^0 = 0.106 V	E^0 = 0.134 V	E^0 = 0.092 V
	n_{50} = 2.0	n_{50} = 1.84	n_{50} = 1.37	n_{50} = 1.02
	n_{max} = 2.10 [20]	n_{max} = 2.05	n_{max} = 1.58	n_{max} = 1.22
KCl 0.05 M		E^0 = 0.121 V	E^0 = 0.142 V	E^0 = 0.101 V
MOPS 0.05 M, pH 7.1		n_{50} = 1.68	n_{50} = 1.25	n_{50} = 1.10
		n_{max} = 1.88	n_{max} = 1.46	n_{max} = 1.17
KCl 0.2 M	E^0 = 0.126 V	E^0 = 0.141 V	E^0 = 0.145 V	E^0 = 0.103 V
MOPS 0.05 M, pH 7.1	n_{50} = 1.55	n_{50} = 1.32	n_{50} = 1.26	n_{50} = 1.04
	n_{max} = 1.83 [20]	n_{max} = 1.47	n_{max} = 1.52	n_{max} = 1.07
$NaNO_3$ 0.05 M		E^0 = 0.124 V	E^0 = 0.142 V	E^0 = 0.091 V
MOPS 0.05 M, pH 7.1		n_{50} = 1.51	n_{50} = 1.27	n_{50} = 0.99
		n_{max} = 1.83	n_{max} = 1.44	n_{max} = 1.02
$NaNO_3$ 0.2 M	E^0 = 0.134 V	E^0 = 0.130 V	E^0 = 0.143 V	E^0 = 0.091 V
MOPS 0.05 M, pH 7.1	n_{50} = 1.40	n_{50} = 1.25	n_{50} = 1.19	n_{50} = 0.98
	n_{max} = 1.70 [20]	n_{max} = 1.54	n_{max} = 1.39	n_{max} = 1.05
HbA in KNO_3 0.2 M, phosphate buffer 0.02 M, pH 7.0	E^0 = 0.177 V			
WE: Pt modified with Brilliant Cresyl Blue	n = 1.4 [32]			
HbA in KNO_3 0.2 M, phosphate buffer 0.02 M, pH 7.0	E^0 = 0.040 V			
WE: Pt modified with Methylene Blue	n = 1.24 [33]			

The concentration of hemoglobin samples was 0.1 mM/heme and the concentration of mediator, $Ru(NH_3)_6Cl_3$, was 0.5 mM. The standard deviation for E^0 was ±3 mV for HbA and αXL-HbA and ±4 mV for βXL-HbA. The standard deviation for n_{50} and n_{max} was between ±0.05 and ±0.10. The values reported are averages of at least three measurements. Literature values for hemoglobin A (SEC, UV–Vis) are provided for comparison.

As seen in Table 2, our experimental values obtained for HbA in the presence of mediator, $Ru(NH_3)_6Cl_3$ agree well with literature data. Slight discrepancies may be due to the way the reported potential was converted from Ag/AgCl to NHE.

Crosslinking of hemoglobin and addition of anions resulted in two trends: 1) shift in formal redox potential, and 2) change in the slope of the Nernst plot. The formal redox potential of αXL-HbA in MOPS 0.05 M is shifted 28 mV positive compared to HbA (Table 2). This shift is consistent with an increased stabilization of the tense (T) conformation brought about by crosslinking reaction. When oxyhemoglobin is crosslinked with DBSF, the modification occurs between the β subunits, which brings stability to the R relative to T conformation. Consequently, the formal redox potential is shifted 14 mV negative for the βXL-HbA as compared to HbA in MOPS 0.05 M (Table 2). The crosslinking at the β–β interface confers rigidity to the hemoglobin molecule to a larger extent than the modification at the α–α interface. However, it was determined from X-ray crystallographic data that the F helix is positioned in a T state-like conformation relative to the heme, the iron ion experiencing the electronic stabilization of the T state [13]. This fact may explain the small negative shift of the formal redox potential, relative to that of HbA.

All hemoglobins (HbA, αXL-HbA and βXL-HbA) had formal redox potential shifted positive by allosteric effectors (anions), although to different extents. Chloride ions had a greater impact at high concentrations (0.2 M) whereas at low concentration (0.05 M), nitrate ions produce a slightly more positive shift in the formal redox potential. As shown in Table 2, making a 0.05 M Cl^- or NO_3^- solution in 0.05 M MOPS shifts the formal redox potential of HbA from 0.106 V to 0.121 V or 0.124 V (15 mV and 18 mV, respectively). Making a 0.2 M Cl^- solution

in 0.05 M MOPS shifts the formal redox potential of HbA from 0.106 V to 0.141 V or 0.130 V (35 mV and 24 mV, respectively). Positive shift in E^0 implies a shift in conformational transition toward the T state.

At molecular level, the conformational shift T→R is attributed to the movement of the α and β chains at the $\alpha_1\beta_2$ and $\alpha_2\beta_1$ interfaces, named as the "switch region", with disruption and formation of hydrogen bonds and salt bridges [1]. Salt bridges also form between positively charged residues at the $\beta_1\beta_2$ interface (known as BPG binding site), His NA2(2), Val NA1(1), His H21(143) and Lys EF6(82), and heterotropic ligands such as 2,3-bisphosphoglycerate, chloride or nitrate ions. Upon oxidation, hydrogen bonds and salt bridges involving C-terminal residues and those within the BPG binding site are broken. The complete movement of the $\alpha_1\beta_1$ and $\alpha_2\beta_2$ dimers is hindered in the presence of anions, and therefore, the equilibrium T↔R is shifted toward the T state [23]. Stabilization of the T conformation indirectly influences the inner-coordination sphere of the Fe porphyrin. As seen in crystallographic [24], resonance Raman [25], and NMR [26] studies, the iron ion does not fully come into the porphyrin plane, and therefore lacks the electronic stabilization conferred by the porphyrin ring [3,5–8]. Lower electron density favors the Fe^{2+} state rather than the Fe^{3+} state thus shifting the formal redox potential positive.

For the native hemoglobin, nitrate and chloride ions differ in their mechanism of binding in the "switch region". Nitrate ions may bond by both salt bridges and by hydrogen bonds, therefore accounting for increased stabilization of the T(deoxy) conformation at low concentrations compared to the low concentration of chloride ions.

The presence of chloride ions caused a small positive shift in the formal redox potential of βXL-HbA, 9 mV ($[Cl^-]$=0.05 M) and 11 mV ($[Cl^-]$=0.2 M), from the value measured in MOPS buffer only, while the presence of nitrate ions had practically no effect on E^0. This is in agreement with the finding of Perutz and Imai [27] and Bonaventura and Bonaventura [28] that human hemoglobin variants and hemoglobins of some species that lack specific positive charges in the central cavity are relatively insensitive to anions. In this experiment the covalent modification is between the ε-amino groups of Lys EF6(82) of the β chains in the central cavity, side chain residues already identified as anion binding sites. The crosslinking reaction removes two positive sites, a fact that explains the small positive shift in formal redox potential with addition of chloride ions. This shift probably arises from the binding of chloride ions to terminal amino groups or histidyl residues that are still accessible following crosslinking reaction.

Similar positive formal redox potential shifts with Cl^- were observed for αXL-HbA. In this case, however NO_3^- also produced positive potential shifts. E^0 shifted 11 mV positive in the presence of 0.2 M KCl and 9 mV positive in the presence of 0.2 M $NaNO_3$ from the value of 134 mV in the absence of allosteric effectors. The concentration of chloride and nitrate ions did not play a significant role in shifting E^0. This is attributed to the fact that the crosslinking reaction of deoxyhemoglobin does not affect the central cavity as much as it does for βXL-HbA.

The Nernst plots for HbA, αXL- and βXL-HbA are sigmoidal and two values of n, one at E^0 (n_{50}) and one at the maximum along the Nernst plot (n_{max}), can be determined according to Eq. (3). Values of n greater than 1 indicate cooperative interactions effecting electron transfer [4,5]. The n_{50} and n_{max} values (Table 2, Fig. 4b) reflect a decrease in cooperativity with increasing ionic strength as noted in the literature [3,5–8,20]. Cooperativity was lower for αXL-HbA and βXL-HbA than for HbA regardless of the direction of the shift in E^0. According to the MWC model [29], maximum cooperativity occurs at E^0, when half of the hemoglobin molecules are in the T and half are in the R conformation. In our experiments, the maximum on the Nernst plots occurred at potentials slightly more positive than E^0. The shift, $\Delta E_n = E_{n_{max}} - E^0$, did not follow any trend with changing experimental conditions (electrolyte type, crosslinking); this shift may be attributed to experimental artifacts. For the purpose of detailed analysis based on the two-state model, n_{max} will be associated with E^0 since n_{max} values are more affected by variation of experimental conditions than n_{50} values.

According to the MWC model [11,29], n_{max} is related to E^0 by

$$n_{max} = 1 + \frac{3(1 - c\alpha_{50})(\alpha_{50} - 1)}{(1 + c\alpha_{50})(\alpha_{50} + 1)} \quad (5)$$

through parameters α_{50}, K_R and K_T where the parameter c is the ratio K_R/K_T. K_R and K_T are the ligand (water molecule and an electron–hole) dissociation constants for the R and T states. Parameter α_{50} is defined as:

$$\alpha_{50} = \frac{\exp\left(E^{0\prime}F/RT\right)}{K_R}. \quad (6)$$

The variation of n_{max} with E^0 follows the trend predicted by MWC model (Fig. 5) for HbA and αXL-HbA (curve 1). In addition to our data (E^0, n_{max}) values obtained by Crumbliss and co-workers are included [12,13]. These data were fit using the values of 0.065 for c and 20 for K_R. Our K_R and c values agree well with those by Perutz et al. [30] (c=0.1 and 12<K_R<20) and Baldwin and Chothia [11] (0.03<c<0.1).

The points corresponding to βXL-HBA are clustered at the right of the fitted curve 1. Several factors may account for this deviation. Chain heterogeneity that results from more than one type of site being oxidized or reduced, or from coupling between sites resulting in negative cooperativity may cause values of n lower than one in the initial stages of the oxidation and reduction processes [5]. The data points for βXL-HbA (curve 2) could be fitted by larger values for K_R (34 instead of 20) and c (0.11 instead of 0.065). The data suggest that crosslinking affects the coordination of water at the heme site, which in turn should play a role in the kinetics of oxidation/reduction and possibly autoxidation. From the definition of K_R, larger value means decreased affinity for water of the ferric ion and decreased tendency for accepting an electron.

K_R and c are not independent variables. They are related through the allosteric constant, L, defined as the ratio of molecules in the T state and R state in the absence of ligand. L changes according to the following equation:

$$L = \frac{(\alpha_{50} - 1)(1 + \alpha_{50})^3}{(1 - c\alpha_{50})(1 + c\alpha_{50})^3} \quad (7)$$

The log L is between 3.8 and 5.5 for αXL-HbA, between 2.1 and 4.5 for HbA, and between −0.4 and 1.0 for βXL-HBA. These values for log L confirmed that crosslinking at the $\alpha_1\alpha_2$ interface stabilizes the T state whereas crosslinking at the $\beta_1\beta_2$ interface stabilizes the R state.

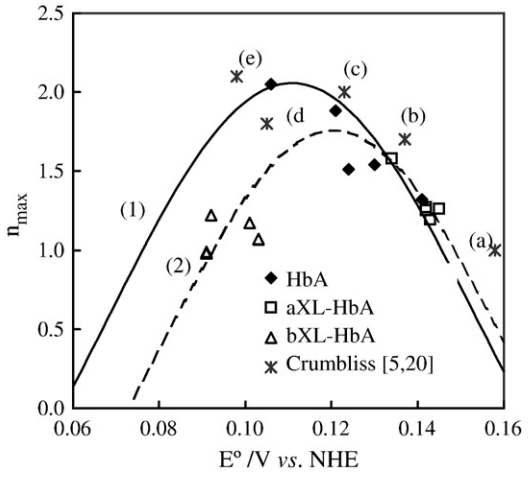

Fig. 5. Maximum in cooperativity, n_{max}, plotted against formal redox potential, E^0, for HbA, αXL-HbA and βXL-HbA for all experimental conditions investigated. Data taken from Table 2 are fitted based on MWC model (Eq. (5)). Curve (1) c=0.065, K_R=20 (through HbA and αXL-HbA data points), curve (2) c=0.11, K_R=38 through βXL-HbA data points. Experimental values (E^0, n_{max}) for HbA obtained by Bonaventura, Crumbliss and co-workers at pH 7.1: [5,6,20] (a) MOPS 0.05 M, $NaNO_3$ 0.2 M with IHP 10-fold excess over heme, (b) MOPS 0.05 M, $NaNO_3$ 0.2 M, (c) MOPS 0.05 M, KCl 0.2 M, (d) MOPS 0.2 M, and (e) MOPS 0.05 M are added for comparisons.

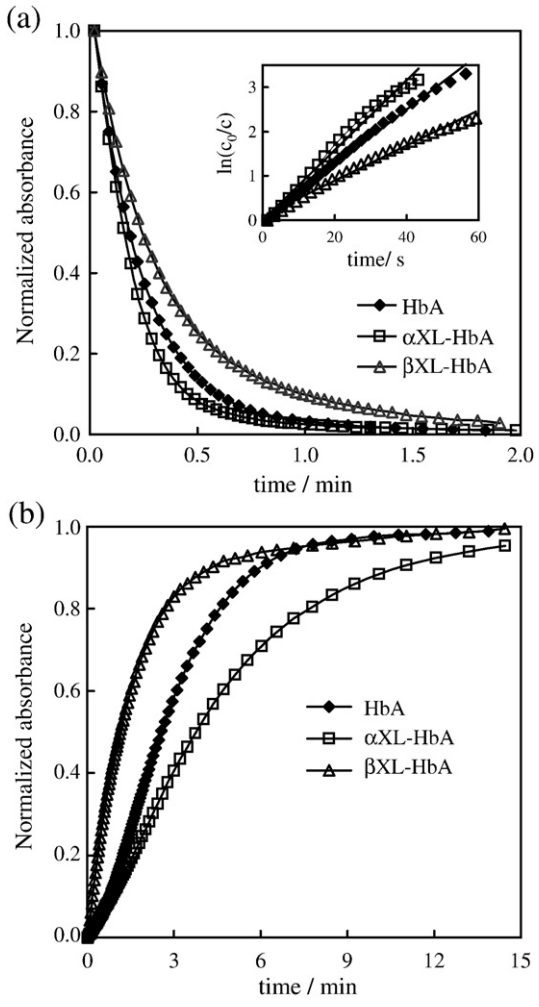

Fig. 6. Time-based measurements for HbA, αXL-HbA and βXL-HbA monitored at 406 nm. Normalized absorbance is defined as $(A_t - A_\infty)/(A_0 - A_\infty)$ for reduction, and as $(A_0 - A_t)/(A_0 - A_\infty)$ for oxidation. Conditions: sample concentration 0.1 mM/heme, 0.5 mM Ru$(NH_3)_6Cl_3$, KCl 0.2 M, MOPS 0.05 M, pH 7.1. (a) Complete reduction (potential stepped from 0.3 V to −0.5 V *vs.* Ag/AgCl). Inset: evaluation of first rate order constants, k_1. (b) Complete oxidation (potential stepped from −0.5 V to 0.3 V *vs.* Ag/AgCl).

3.2. Kinetics

Time-based monitoring of reduction and oxidation of hemoglobins in the presence of mediator, Ru$(NH_3)_6Cl_3$ was performed by applying large potential steps from −0.5 V to +0.3 V *vs.* Ag/AgCl and vice versa, as illustrated in Fig. 6. Similar behavior was observed for HbA and crosslinked hemoglobins when the same buffer/electrolyte system was used. For all systems that have chloride or nitrate dissolved in 0.05 M MOPS buffer, the reduction curves are hyperbolic (Fig. 6a) while the oxidation curves present an inflection point (Fig. 6b). The rate of oxidation increases with the progress of the reaction, the change being especially evident in the initial stages. Oxidation is slowed by addition of salts especially by the presence of nitrate, while the reduction reaction proceeds faster in the presence of the above anions. The same trend was found for αXL- and βXL-HbA.

Cross-reaction rate constants (k_{12}) for reduction were calculated by dividing the experimental pseudo-first order rate constant (k_1) by the concentration of mediator. Reduction of hemoglobins in the presence of Ru$(NH_3)_6Cl_3$ with addition of salts follows a first order mechanism. At every applied potential during the reduction process, the calculated concentration of the mediator exceeded that of the hemoglobins. The rate constants displayed in Table 3 as k_1 are pseudo-first order rate constants with respect to hemoglobin.

The electrochemical reduction of hemoglobin molecules, as measured by k_{12}, is driven by the difference in the formal redox potential between the acceptor (being reduced) and the donor (being oxidized) species ($\Delta E^0 = E^0$acceptor $- E^0$donor) according to Marcus cross-relationship [31]:

$$\log k_{12} = \frac{1}{2}\left(\log k_{11} + \log k_{22} + \frac{nF}{2.3RT}\Delta E^0\right) \quad (8)$$

where k_{11}, and k_{22} are the self-exchange rate constants of $Ru(NH_3)_6^{3+/2+}$ and hemoglobins ($Fe^{3+/2+}$), respectively.

Since the quantity ΔE^0 is positive when hemoglobin is reduced, reduction generally proceeds faster than oxidation. Because ΔE^0 is electrolyte-dependent the rate also depends, slightly, on electrolyte composition. Other terms significant in describing the rate of the mediated hemoglobin reduction reaction are k_{11}, and k_{22}, the self-exchange rate constants of $Ru(NH_3)_6^{3+/2+}$ and hemoglobins ($Fe^{3+/2+}$), respectively.

The k_{22} values refer to a complete sequence of microscopic steps involved in electron transfer such as: access of water to the heme site (quantitatively expressed by K_R), ease of change in doming of the porphyrin ring upon addition or removal of water, and quaternary conformational transition. The linear regression analysis based on Eq. (8), using the value of 4×10^3 M^{-1} s^{-1} for k_{11} of $Ru(NH_3)_6^{3+/2+}$, was excellent for HbA suggesting that the concerted water (ligand) dissociation and electron transfer required for the application of Marcus theory is plausible. A value of 0.191 ± 0.017 M^{-1} s^{-1} was obtained for the native HbA.

Our k_{22} values obtained for hemoglobins are much larger than the self-exchange rate constants calculated from Marcus theory from heterogeneous rate constants, k_s, for the electron transfer between heme proteins and an electrode surface obtained by electrochemical

Table 3
Experimental pseudo-first rate order constant for reduction, k_1, and self-exchange rate constants at infinite ionic strength, $k_{22\infty}$, calculated with Marcus cross-relationship (Eq. (8)) for HbA, αXL-HbA and βXL-HbA

System	HbA			αXL-HbA			βXL-HbA		
	ΔE^0, V	k_1, s^{-1}	$k_{22\infty}$, M^{-1} s^{-1}	ΔE^0, V	k_1, s^{-1}	$k_{22\infty}$, M^{-1} s^{-1}	ΔE^0, V	k_1, s^{-1}	$k_{22\infty}$, M^{-1} s^{-1}
KCl 0.05 M MOPS 0.05 M I=0.072 M	0.067	0.037	0.137	0.087	0.047	0.096	0.046	0.026	0.138
KCl 0.2 M MOPS 0.05 M I=0.222 M	0.094	0.050	0.096	0.097	0.064	0.103	0.055	0.038	0.180
$NaNO_3$ 0.05 M MOPS 0.05 M I=0.072 M	0.068	0.033	0.104	0.086	0.054	0.130	0.034	0.028	0.265
$NaNO_3$ 0.2 M MOPS 0.05 M I=0.222 M	0.080	0.047	0.109	0.093	0.083	0.199	0.042	0.031	0.207

The driving potential, ΔE^0, the difference in the formal redox potential of the acceptor and donor species, was calculated with the values listed in Tables 1 and 2.

methods. These estimates vary from 1.37×10^{-10} M^{-1} s^{-1} (Pt modified with Brilliant Cresyl Blue) [32] to 3.9×10^{-5} M^{-1} s^{-1} (Pt modified with Methylene Green) [33] probably because of impurities such as oxygen-bound proteins not properly removed, and use of incompatible electrode surfaces which become passivated by denaturated proteins. Recently k_{22} values of 0.144±0.009 M^{-1} s^{-1} were obtained for hemoglobin by using gold electrode modified with ω-hydroxyalkane thiols [34]. DDAB (didodecyldimethyl-ammonium bromide) modified electrode surfaces yielded self-exchange rate constants for myoglobin from 0.009 to 0.049 and to 0.121 M^{-1} s^{-1}, values that are comparable to ours and to spectroscopic measurements on similar protein systems in which heme is not forced to planarity [35]. These comparisons suggest that the values we obtained are accurate reflections of the magnitude of self-exchange rate constants for our three hemoglobin systems.

For both crosslinked hemoglobins, the linear fit was poor. Lack of fit to the Marcus cross-reaction implied that the concerted motion of water and an electron–hole does not occur. The k_{22} values obtained by linear regression analysis were 0.012±0.004 M^{-1} s^{-1} for αXL-HbA and 0.299±0.096 M^{-1} s^{-1} for βXL-HbA. The results of the kinetic analysis are consistent with the results obtained by modeling the data according to the MWC theory. That analysis indicated that the major impact of crosslinking is not only on the electron density at the iron site but also on the steric changes affecting the binding of water.

3.3. Autoxidation

In the autoxidation reaction, the concentration of oxyhemoglobin was found to decay exponentially in time for all hemoglobins (Fig. 7), and first order autoxidation rate constants (Table 4) were obtained by a similar treatment of data as for those from electrochemical reduction (Eq. (4)).

The data show that αXL-HbA (T conformation stabilized) autoxidizes faster than βXL-HbA, which has the R (oxy) conformation stabilized by crosslinking, and faster than native hemoglobin in agreement with the literature [36]. The increased autoxidation rate of the αXL-HbA is consistent with the suggestion that autoxidation proceeds via deoxyhemoglobin and that hemoglobin molecules that have the T (deoxy) conformation stabilized would autoxidize faster [37]. Addition of chloride and nitrate, which tend to stabilize the T (deoxy) conformation, caused autoxidation to be faster for all three compounds (Table 4). One explanation for this relates to the role of water in autoxidation. This suggested mechanism has oxygen binding

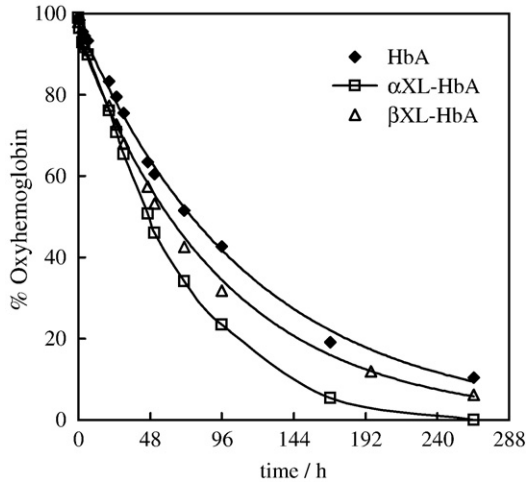

Fig. 7. Autoxidation of HbA, αXL-HbA and βXL-HbA in $NaNO_3$ 0.2 M, MOPS 0.05 M, pH 7.1 at room temperature monitored as decay of percent of oxyhemoglobin in time. Initial concentration of samples was 0.1 mM/heme.

Table 4
Apparent autoxidation rates for HbA, αXL-HbA and βXL-HbA determined at room temperature (22±1 °C), pH 7.1

System	HbA	αXL-HbA	βXL-HbA
	$100\times k_{app}$, h^{-1}	$100\times k_{app}$, h^{-1}	$100\times k_{app}$, h^{-1}
MOPS 0.05 M KCl 0.05 M	0.44	0.65	0.56
MOPS 0.05 M KCl 0.2 M	0.45	0.68	0.62
MOPS 0.05 M $NaNO_3$ 0.05 M	0.79	1.18	0.96
MOPS 0.05 M $NaNO_3$ 0.2 M MOPS 0.05 M	0.48	0.71	0.68
	0.89	1.47	1.06

The listed values are averages of at least two measurements. Initial concentration of oxyhemoglobins was 0.1±0.01 mM/heme.

to the ferrous ion in the heme pocket to form a ferriheme-superoxide complex which is displaced by water in a nucleophilic substitution (SN_2) [37]:

$$HbA(Fe^{2+})\text{–}O_2 \rightarrow HbA(Fe^{3+}) - - O_2^- \qquad (9-1)$$

$$HbA(Fe^{3+}) - - O_2^- + H_2O \rightarrow HbA(Fe^{3+})\text{–}H_2O + O_2^- \qquad (9-2)$$

Superoxide anion released from the ferriheme-suproxide complex is either scavenged by the superoxide dismutase present in the red blood cells or further reacts with water to form hydroxide anion and the free hydroxyl radical [37].

Yasuda et. al. found that increased hydrophilicity at the heme site allows weak nucleophiles (H_2O, OH^-, or Cl^-) to enter the heme pocket from the surrounding solvent and displace superoxide anion, with concomitant formation of methemoglobin [38]. Site directed mutagenesis studies carried out by Brantley et al. concluded that the rate of autoxidation could be dramatically increased by increasing the polarity of the heme pocket or by increasing the net anionic charge at the protein surface in the vicinity of the heme [39].

Hemoglobin variants with weak affinity for water would be expected to have slow reaction rate [40]. The βXL-HbA has a large dissociation constant for water (K_R value) and therefore reduced access of water in the heme pocket to drive the reaction. This fact may be related to a reduced overall rate of autoxidation of the βXL-HbA compared to αXL-HbA. Unfortunately, the converse is not true. The faster autooxidation of αXL-HbA (compared to HbA) cannot be explained by a K_R less than that of HbA. Nor can the faster rate of oxidation be explained by shifts in the formal potential as they are in the wrong direction. This suggests, in the context of the ferriheme-superoxide model, that crosslinking in the alpha form might alter accessibility of the heme group to oxygen. This suggestion is consistent with the suggestion that the location of the crosslinking group on the hemoglobin tetramer can differentially affect the free radical reactivity of the protein. This finding was substantiated by studies involving cultured endothelial cells [41].

Clear correlations between autoxidation rates and formal redox potentials or conformations of native, alpha, and beta-fumarate crosslinked hemoglobins were not found. This is in agreement with other published studies related to autoxidation and oxygen binding properties of chemically and genetically-modified hemoglobins. While oxygen binding could be controlled by design, autoxidation could not, supposedly because of the difficulty encountered in the assignment of R and T states to the α and β subunits within the recombinant tetramer [39]. The chemical mechanism of oxygen dissociation and accessibility of oxygen radicals and/or water to the heme site may control autoxidation. The chemical mechanism would, therefore, prevail over thermodynamic factors such as formal redox potential of heme group.

4. Conclusions

The spectroelectrochemical method employed for this study of native, alpha-, and beta-crosslinked hemoglobins proved to be very sensitive in detecting small variations of formal redox potential, E^0, parameters n_{max} and n_{50} with crosslinking and with addition of allosteric effectors (chloride and nitrate ions). The formal redox potential of αXL-HbA (which retained the tense conformation following crosslinking) shifted positive compared to native HbA. The formal redox potential of βXL-HbA (which retained the relaxed conformation following crosslinking) shifted negative compared to HbA. Cooperativity was reduced for both crosslinked hemoglobins. Addition of chloride and nitrate ions caused the formal redox potential of HbA and αXL-HbA to shift positive, indicating stabilization of the ferrous hemoglobin and tense conformation. The data points (E^0, n_{max}) were modeled by the MWC formalism with the same values for K_R and c for HbA and αXL-HbA and different set of K_R and c values for βXL-HbA suggesting that the crosslinking at the $\beta_1\beta_2$ interface confers a higher degree of rigidity to hemoglobin molecule.

The self-exchange rate constants, k_{22}, derived from the evaluation of the rate constants for full reduction refer to a complete sequence of microscopic steps involved in electron transfer both at the heme site and on the overall conformation of the hemoglobin molecule. βXL-HbA was found to have the largest value of k_{22} followed by HbA and by αXL-HbA.

The autoxidation rate constants could not be predicted by formal redox potentials or by self-exchange rate constants. The αXL-HbA, which retains much of the T conformation, presented the highest tendency for autoxidation. The βXL-HbA, which retains the R conformation showed slower autoxidation rate than αXL-HbA but not slower than HbA. Our hypothesis is that the chemical mechanism of oxygen dissociation and accessibility of water and other nucleophilic agents to the heme site may control autoxidation rates. The chemical mechanism would, therefore, prevail over thermodynamic factors such as the formal redox potential of heme($Fe^{3+/2+}$).

Acknowledgements

This work was supported by the Loyola University Chicago, Loyola University Teaching Fellowship, Arthur A. Schmitt Fellowship Foundation, and an NSF-Research Experience for Undergraduates grant (0243825). We acknowledge Baxter Healthcare Corporation for the sample of αXL-HbA generously provided.

References

[1] M.F. Perutz, G. Fermi, B. Luisi, B. Shaanan, R. Liddington, Stereochemistry of cooperative mechanisms in hemoglobin, Acc. Chem. Res. 20 (1987) 309–321.
[2] C.C. Winterbourn, Free-radical production and oxidative reactions of hemoglobin, Environ. Health Perspect. 64 (1985) 321–330.
[3] C.H. Taboy, C. Bonaventura, A.L. Crumbliss, Concentration-dependent effects of anions on the anaerobic oxidation of hemoglobin and myoglobin, J. Biol. Chem. 275 (2000) 39048–39054.
[4] C.H. Taboy, C. Bonaventura, A.L. Crumbliss, Spectroelectrochemistry of heme proteins: effects of active-site heterogeneity on Nernst plots, Bioelectrochem. Bioenerg. 48 (1999) 79–86.
[5] K.M. Faulkner, C. Bonaventura, A.L. Crumbliss, A spectroelectrochemical method for differentiation of steric and electronic effects in hemoglobins and myoglobins, J. Biol. Chem. 270 (1995) 13604–13612.
[6] C. Bonaventura, S. Tesh, K.M. Faulkner, D. Kraiter, A.L. Crumbliss, Conformational fluctuations in deoxy hemoglobin revealed as a major contributor to anionic modulation of function through studies of the oxygenation and oxidation of hemoglobin A0 and hemoglobin deer lodge β2(NA2)His-Arg, Biochemistry 37 (1998) 496–506.
[7] C. Bonaventura, C.H. Taboy, P.S. Low, R.D. Stevens, C. Lafon, A.L. Crumbliss, Heme redox properties of *S*-nitrosated hemoglobin A0 and hemoglobin S. Implications for interactions of nitric oxide with normal and sickle red blood cells, J. Biol. Chem. 277 (2002) 14557–14563.
[8] C. Bonaventura, G. Godette, S. Tesh, D.E. Holm, J. Bonaventura, A.L. Crumbliss, L.L. Pearce, J. Peterson, Internal electron transfer between hemes and Cu(II) bound at cysteine β93 promotes methemoglobin reduction by carbon monoxide, J. Biol. Chem. 274 (1999) 5499–5507.
[9] J.A. Walder, R.Y. Walder, A. Arnone, Development of antisickling compounds that chemically modify hemoglobin S specifically within the 2,3-diphosphoglycerate binding site, J. Mol. Biol. 141 (1980) 195–216.
[10] R. Chatterjee, E.V. Welty, R.Y. Walder, S.L. Pruit, P.H. Rogers, A. Arnone, J.A. Walder, Isolation and characterization of a new hemoglobin derivative crosslinked between the α chains (lysine 99 α1–lysine 99 α2), J. Biol. Chem. 261 (1986) 9929–9937.
[11] J. Baldwin, C. Chothia, Hemoglobin: the structural changes related to ligand binding and its allosteric mechanism, J. Mol. Biol. 129 (1979) 175–220.
[12] S.R. Snyder, E.V. Welty, R.Y. Walder, L.A. Williams, J.A. Walder, HbXL99 α: a hemoglobin derivative that is cross-linked between the α subunits is useful as a blood substitute, Proc. Natl. Acad. Sci. U. S. A. 84 (1987) 7280–7284.
[13] E.J. Fernandez, C. Abad-Zapatero, K.W. Olsen, Crystal structure of Lys β182–Lys β282 crosslinked hemoglobin: a possible allosteric intermediate, J. Mol. Biol. 296 (2000) 1245–1256.
[14] A.M. Dozy, E. Kleihauer, T.H.J. Huisman, Heterogeneity of hemoglobin. XIII. Chromatography of various human and animal hemoglobin types on diethylaminoethyl-Sephadex, J. Chromatogr. 32 (1968) 723–727.
[15] C.C. Winterbourn, Reactions of superoxide with hemoglobin, in: R.A. Greenwald (Ed.), CRC Handbook of Methods for Oxygen Radical Research, CRC, Boca Raton FA, 1985, pp. 137–141.
[16] F.L. White, K.W. Olsen, Effects of crosslinking on the thermal stability of hemoglobin. I. The use of bis(3,5-dibromosalicyl) fumarate, Arch. Biochem. Biophys. 258 (1987) 51–57.
[17] J.A. Walder, R.H. Zaugg, R.Y. Walder, J.M. Steele, I.M. Klotz, Disapirins that crosslink β chains of hemoglobin: bis(3,5-dibromosalicyl) succinate and bis(3,5-dibromosalicyl) Fumarate, Biochemistry 18 (1979) 4261–4270.
[18] A. Riggs, Preparation of blood hemoglobins of vertebrates, Methods Enzymol. 76 (1981) 5–29.
[19] W.R. Heineman, B.J. Norris, J.F. Goelz, Measurement of enzyme ′ values by optically transparent thin layer electrochemical cells, Anal. Chem. 47 (1975) 79–84.
[20] K.M. Faulkner, C. Bonaventura, A.L. Crumbliss, A spectroelectrochemical method for evaluating factors which regulate the redox potential of hemoglobins, Inorg. Chim. Acta 226 (1994) 187–194.
[21] W.R. Heineman, M.L. Meckstroth, B.J. Norris, C.-H. Su, Optically transparent thin layer electrode techniques for the study of biological redox systems, Bioelectrochem. Bioenerg. 6 (1979) 577–585.
[22] E.A. Blubaugh, A.M. Yacynych, W.R. Heineman, Thin-layer spectroelectrochemistry for monitoring kinetics of electrogenerated species, Anal. Chem. 51 (1979) 561–566.
[23] K. Imai, Analyses of oxygen equilibria of native and chemically modified human adult hemoglobins on the basis of Adair's stepwise oxygenation theory and the allosteric model of Monod, Wyman, and Changeux, Biochemistry 12 (1973) 798–808.
[24] J.V. Kilmartin, Interaction of inositol hexaphosphate with methemoglobin, Biochem. J. 133 (1973) 725–733.
[25] J.M. Friedman, Time-resolved resonance raman spectroscopy as probe of structure, dynamics, and reactivity in hemoglobin, in: J. Everse, K.D. Vendegriff, R.M. Winslow (Eds.), Methods in Enzymology: Hemoglobins, Vol. 232, Academic Press, San Diego, 1994, pp. 205–231.
[26] M.R. Busch, C.E. Ho, Effects of anions on the molecular basis of the Bohr effect of hemoglobin, Biophys. Chem. 37 (1990) 313–322.
[27] M.F. Perutz, K. Imai, Regulation of oxygen affinity of mammalian hemoglobins, J. Biol. Chem. 136 (1980) 183–191.
[28] C. Bonaventura, J. Bonaventura, Anionic control of hemoglobin function, in: W.S. Caughey (Ed.), Biochemical and Clinical Aspects of Hemoglobin Abnormalities, Academic Press, New York, 1978, pp. 647–663.
[29] J.J. Monod, J. Wyman, J.P. Changeux, On the nature of allosteric transitions: a plausible model, J. Mol. Biol. 12 (1965) 88–118.
[30] M.F. Perutz, A.R. Fersht, S.R. Simon, G.C.K. Roberts, Influence of globin structure on the state of the heme. II. Allosteric transitions in methemoglobin, Biochemistry 12 (1974) 2174–2186.
[31] R.A. Marcus, Theory of electron-transfer reactions. VI. Unified treatment for homogeneous and electrode reactions, J. Chem. Phys. 43 (1965) 679–701.
[32] S. Dong, Y. Zhu, S. Song, Electrode processes of hemoglobin at a platinum electrode covered by Brilliant Cresyl Blue, Bioelectrochem. Bioenerg. 21 (1989) 233–243.
[33] Y. Zhu, S. Dong, Rapid redox reaction of hemoglobin at methylene green modified platinum electrode, Electrochim. Acta 35 (1990) 1139–1143.
[34] J.L. Blankman, N. Shahzad, C.J. Miller, R.D. Guiles, Direct voltammetric investigation of the electrochemical properties of human hemoglobin: relevance to physiological redox chemistry, Biochemistry 39 (2000) 14806–14812.
[35] A.E. Nassar, W.S. Willis, J.F. Rusling, Electron transfer from electrodes to myoglobin: facilitated in surfactant films and blocked by adsorbed biomacromolecules, Anal. Chem. 67 (1995) 2386–2392.
[36] T. Yang, K.W. Olsen, The effect of crosslinking by bis(3,5-dibromosalicyl) fumarate on the autoxidation of hemoglobin, Biochem. Biophys. Res. Commun. 163 (1989) 733–738.
[37] W.J. Wallace, R.A. Houtchens, J.C. Maxwell, W.S. Cayghey, Mechanism of autooxidation for hemoglobins and myoglobins. Promotion of production by protons and anions, J. Biol. Chem. 257 (1982) 4966–4977.
[38] J.P. Yasuda, T. Ichikawa, M. Tsuruga, A. Matsuoka, Y. Sugawara, K. Shikama, The α1 β1 contact of human hemoglobin plays in a key role in stabilizing the bound dioxygen. Further evidence from the iron valency hybrids, Eur. J. Biochem. 269 (2002) 202–211.
[39] R.E. Brantley Jr., S.J. Smerdon, A.J. Wilkinson, E.W. Singleton, J.S. Olson, The mechanism of autooxidation of myoglobin, J. Biol. Chem. 268 (1993) 995–7010.
[40] W.J. Wallace, J.C. Maxwell, W.S. Caughey, Role for chloride in the autoxidation of hemoglobin under conditions similar to those in erythrocytes, FEBS Lett. 43 (1974) 33–36.
[41] J. Simoni, G. Simoni, C.D. Lox, M. Feola, Reaction of human endothelial cells to bovine hemoglobin solutions and tumor necrosis factor, Artif. Cells Blood Substit. Immobil. Biotechnol. 22 (1994) 399–413.